Dielectric matrices in semiconductors: A direct approach

Andrzej Fleszar and Raffaele Resta*
Scuola Internazionale Superiore di Studi Avanzati, 34014 Trieste, Italy
(Received 19 March 1984; revised manuscript received 28 August 1984)

A new method for the evaluation of dielectric screening matrices in semiconductors is proposed. The present method is direct, in the sense that it avoids the use of slowly convergent perturbation sums, just by treating the crystal with a built-in perturbation as a new system. The several advantages of this approach with respect to previous ones are discussed. As a first application of the method, we calculate the random-phase approximation (RPA) dielectric matrices of Si and GaAs at the Γ, X, and L points; the results show the effectiveness and accuracy of the method. The possibility of extending beyond RPA is also discussed.

I. INTRODUCTION

The first-principles theory of the electronic dielectric response in real solids has attracted much interest in recent years.[1-4] The theory can be compared against experimental data—most directly in connection with phonons—but also gives a thorough understanding of basic (and nonmeasurable) features; for this reason, it is essential to the formulation of realistic models.

Within linear regimes, the response is described by the dielectric matrix.[1,3] Calculations for real materials have been possible only in recent times, starting from the Adler-Wiser[5] random-phase approximation (RPA) approach. Such calculations have proven to be quite elaborate,[6] even if a major simplification has been successfully reached[7] with the use of the mean-value point technique for Brillouin-zone (BZ) integration.[8-10] Two basic features which make such calculations extremely time consuming are the slow convergence of perturbation sums and the need of evaluating one by one the independent dielectric matrix elements. Because of the above reasons, numerical results are available for a few materials only[1-3,7,11] and mostly at the BZ center ($\vec{q}=0$ or $\vec{q}\to 0$).

In this work we present an alternative approach to the evaluation of dielectric matrices. We call it the "direct" RPA, by contrast with the "standard" RPA,[5] and by analogy with recent direct phonon calculations.[12-16] Within such an approach, one calculates a new ground state of the solid with frozen-in perturbation, and evaluates the response as the difference of perturbed minus unperturbed quantities. The use of perturbation theory and slowly convergent perturbation sums is avoided; furthermore, a whole column of the dielectric matrix is calculated at a time.

As a test, we apply our method to Si and GaAs. In order to get a quite accurate check of the present method, we have chosen to work within exactly the same framework as in Refs. 7 and 11, whose complete results are available to us in a computer-usable format. For this reason, our starting band structure is the Cohen-Bergstresser[17] one, obtained through the empirical pseudopotential method. This is the same as in Refs. 7 and 11, whose $\vec{q}=0$ standard RPA results we reproduce here almost identically with much smaller computational effort. Then we are able to go beyond and we calculate, at exactly the same level of accuracy, the dielectric matrices at the X and L points, thus supplementing the Γ results previously published.[7,11] In the case of Si, we compare the main screening features of our first-principle results against some of the available model dielectric matrices; this is done here using the concept of dielectric band structure (DBS), proposed some years ago by Baldereschi and Tosatti[18] and which proves very useful for the purpose.

The present method is indeed a way to evaluate the independent-particle polarizability; therefore it can be straightforwardly applied beyond RPA, to calculate the local-density-functional (LDF) dielectric response according to a well-known prescription.[13,19] Since LDF theory predicts quite good frozen-phonon frequencies,[13,14] we expect LDF dielectric matrices from self-consistent pseudopotentials to also be very accurate in lattice dynamics. In this paper, which is a method one, we prefer not to use such a pseudopotential, for the reasons explained above.

Section II contains the theory of the direct RPA method, as applied to the calculation of the dielectric matrix. In Sec. III, several features related to practical implementation are discussed. In Sec. IV we present numerical results for Si and GaAs. In Sec. V the DBS analysis is performed to compare with some models. In Sec. VI we analyze conclusions and perspectives.

II. DIRECT RPA METHOD

The response of a polarizable medium to a given bare electrostatic potential $\phi_0(\vec{r})$ is described, within the linear theory, by

$$\phi(\vec{r})=\int d\vec{r}\,\epsilon^{-1}(\vec{r},\vec{r}\,')\phi_0(\vec{r}\,') , \tag{1}$$

where ϕ is the screened electrostatic potential and the operator ϵ^{-1} contains all the information about the linear dielectric response of the medium. In compact notations we write Eq. (1) as

$$\phi=\epsilon^{-1}\phi_0 . \tag{2}$$

We use a.u. ($e^2=m_e=\hbar=1$) throughout. The total self-

consistent one-electron Hamiltonian is

$$H = H_0 + \delta V \,, \tag{3}$$

where H_0 is the unperturbed one, and at the RPA level,

$$\delta V = -\phi \,. \tag{4}$$

The basic quantity to deal with is the independent-particle polarizability, which is the linear density response to the *total* potential acting on electrons:

$$n^{(1)} = \chi_0 \delta V \,. \tag{5}$$

The RPA inverse of ϵ^{-1} is then in operator form:

$$\epsilon = 1 - v_C \chi_0 \,, \tag{6}$$

where v_C is the Coulomb potential; since in a periodic solid v_C and χ_0 do not commute, ϵ is not Hermitian. For computational and displaying purposes it is better to refer to the Hermitian operator $\tilde{\epsilon}$, simply related to ϵ by

$$\tilde{\epsilon} = v_C^{-1/2} \epsilon v_C^{1/2} = 1 - v_C^{1/2} \chi_0 v_C^{1/2} \,, \tag{7}$$

which has been widely used in previous literature on the subject.[1,2,7,11]

We have summarized up to now the features which are common to the standard RPA and to the present approach. The basic difference is the way in which the independent-particle polarizability χ_0 is evaluated.

Within the standard RPA, first-order perturbation theory is used to obtain the wave functions of the perturbed Hamiltonian, Eq. (3), linearly in δV. With these wave functions the first-order change in the electron density is evaluated and an expression for χ_0 is found from Eq. (5); it only contains eigenvalues and eigenfunctions of the unperturbed Hamiltonian H_0.

The direct RPA we are proposing in this paper consists of directly solving for the eigenfunctions of the perturbed Hamiltonian, Eq. (3), without use of perturbation theory. The perturbation density is found by difference with the unperturbed case. The calculation is performed with a number of independent δV's sufficient to reconstruct the desired features of χ_0, through Eq. (5), and sufficiently small to ensure linearity. The present approach is inspired by recent direct solid-state calculations with built-in perturbations, such as frozen phonons[12] and other ones,[13–16,4] but at variance with them it does *not* require self-consistency in the perturbed case, since δV is already the total (screened) potential.

Now, we switch to reciprocal space. We use the following notations throughout for the Fourier transform of any function:

$$f(\vec{r}) = (2\pi)^{-3} \sum_{\vec{G}} \int_{\mathrm{BZ}} d\vec{q}\, f(\vec{q}+\vec{G}) e^{-i(\vec{q}+\vec{G})\cdot\vec{r}} \,, \tag{8}$$

where $\vec{G}$ are reciprocal-lattice vectors and $\vec{q}$ is within the BZ. In a periodic solid, the operators dealt with above are invariant under lattice translation and assume in reciprocal space a matrix form. The matrix indices are reciprocal vectors and the matrix elements depend parametrically on $\vec{q}$. For instance, Eq. (5) reads

$$n^{(1)}(\vec{q}+\vec{G}) = \sum_{\vec{G}'} \chi_0(\vec{q}+\vec{G}, \vec{q}+\vec{G}') \delta V(\vec{q}+\vec{G}') \,. \tag{9}$$

The Hermitian dielectric matrix (HDM) is obtained from Eq. (10), which reads

$$\tilde{\epsilon}(\vec{q}+\vec{G}, \vec{q}+\vec{G}') = \delta_{\vec{G},\vec{G}'} - \frac{4\pi}{|\vec{q}+\vec{G}||\vec{q}+\vec{G}'|} \times \chi_0(\vec{q}+\vec{G}, \vec{q}+\vec{G}') \,. \tag{10}$$

The $\vec{G} \neq \vec{G}'$ HDM elements are responsible for "umklapp" effects in the response, which are generally referred to as local-field effects;[1] they are due to lattice periodicity, and are vanishing in a homogeneous system, such as the electron gas.

The starting point of all the previous HDM calculations, according to the best of the authors' knowledge, is the standard RPA expression for χ_0, first given by Adler and Wiser[5]

$$\chi_0(\vec{q}+\vec{G}, \vec{q}+\vec{G}') = -\frac{4}{(2\pi)^3} \sum_{v,c} \int_{\mathrm{BZ}} d\vec{k} \frac{\langle \vec{k}+\vec{q}, c \,|\, e^{i(\vec{q}+\vec{G})\cdot\vec{r}} \,|\, \vec{k}, v \rangle \langle \vec{k}, v \,|\, e^{-i(\vec{q}+\vec{G}')\cdot\vec{r}} \,|\, \vec{k}+\vec{q}, c \rangle}{E_c(\vec{k}+\vec{q}) - E_v(\vec{k})} \tag{11}$$

in terms of Bloch functions and band energies of H_0. Such calculations are quite lengthy, owing basically to the slow convergence of the summation in (11) over the conduction bands. This main problem is avoided within the present approach, where we only use valence wave functions of the perturbed and unperturbed crystal, as explained above. The authors of Refs. 7 and 11, who made full use of symmetry at the Γ point, found the standard RPA calculation still quite heavy. The symmetry benefit applies to our direct RPA calculation too, as explained below. Besides computer time, programming time is also important: The standard RPA requires *ad hoc* manipulation of matrix elements appearing in Eq. (11), which is avoided here.

The essence of our method is as follows: we switch on one monochromatic δV at a time, having a single nonvanishing component at the vector $\vec{q}+\vec{G}'$. We diagonalize the perturbed Hamiltonian and find the perturbation electron density; within the linear regime, this density has nonvanishing Fourier components only at the umklapp vectors $\vec{q}+\vec{G}$. Those components give us, from Eq. (9), one entire column of χ_0 for each monochromatic perturbation. The HDM is Hermitian (and real in centrosymmetric solids), as clearly appears in Eqs. (10) and (11). Within our scheme, it does not come out Hermitian by construction, so we have a very simple accuracy test for the method. For special $\vec{q}$ vectors the number of independent perturbations to be considered is greatly reduced by point symmetry (see below).

III. CALCULATIONS

Some features concerning the practical implementation of the above concepts to dielectric matrix calculations in semiconductors are separately discussed in the following.

A. Hermiticity

When the perturbation potential δV has a single Fourier component at $\vec{q}+\vec{G}'$, i.e., in real space

$$\delta V(\vec{r})=ve^{-i(\vec{q}+\vec{G}')\cdot\vec{r}} \tag{12}$$

the total Hamiltonian (3) is no longer Hermitian. This problem is easily circumvented by considering the density response to sine and cosine perturbations separately, each of which is real. The linear response to the perturbation (12) is then easily reconstructed. We notice at this point that in centrosymmetric materials a cosine perturbation always induces an even response, while a sine perturbation induces an odd response only within the *linear* regime. In a centrosymmetric material, the linear response to a cosine can be expanded as a Fourier cosine series and analogously for the sines, and this is the reason why we obtain a real symmetric χ_0. In noncentrosymmetric materials there are mixed sine-cosine responses, which are responsible for complex elements in the Hermitian matrix χ_0.

B. Linearity

Any linear response is, by definition, the linear term in the response to a vanishingly small perturbation. In other words, it is a functional derivative which we are evaluating in this work as a finite incremental ratio; we are therefore interested in choosing the strength of the perturbation v as small as possible. But since the (small) perturbation density is obtained as the difference of two large quantities, we are faced with a cancellation problem. It turns out that there is a large range of strengths which are small enough to induce linear response, although large enough to ensure cancellation causes no harm. This is in agreement with previous successful calculations for frozen *harmonic* phonons[12–14] where basically the same problem exists. Within this work, we have performed a preliminary study and we have chosen a value of $v=5\times10^{-5}$ hartree as the amplitude of our sine and cosine perturbations δV. The wisdom of this choice was assessed by several *a posteriori* checks on the results. Two of them have been already mentioned (Hermiticity of χ_0 or equivalently of $\tilde{\epsilon}$; odd response to odd perturbations in centrosymmetric crystals); others will be discussed below.

C. Supercells

The perturbed Hamiltonian, Eq. (3), when $\vec{q}=0$ has the same lattice periodicity as the unperturbed crystal; but when $\vec{q}\neq0$ this is no longer true. Since the one-electron states are easily obtained for a periodic Hamiltonian, we are forced to use some special $\vec{q}$ values, such that the perturbed Hamiltonian is periodic over a suitable supercell and the $\vec{q}+\vec{G}$ vectors (for any $\vec{G}$) are among the reciprocal vectors of the new system (crystal plus perturbation). The feature is exactly the same as in the context of phonons[12–16] and will not be discussed further here. In the calculations presented in this work we deal with the Γ point (no supercell) and with the X and L points (supercell repeating twice the elementary cell in suitable directions).

A first comment concerns the zone-center case. A constant potential induces zero density response, of course, and our approach only gives the $\vec{G}\neq0$ *and* $\vec{G}'\neq0$ elements of χ_0 and ϵ; the missing elements are only defined in the $\vec{q}\to0$ limit and would require larger and larger supercells within the present scheme, while they are easily obtained within the standard RPA scheme.[7,11] An extension of the method of Ref. 4 could also possibly be implemented within the present approach.

A second comment concerns the zone-boundary cases, either X or L. We continue to use the $\vec{G}$ letter with the meaning of reciprocal vectors of the original lattice; then the reciprocal vectors of the superlattice can be partitioned in two sets: the $\vec{G}$ ones, and those having the form $\vec{q}+\vec{G}$. The unperturbed density has nonvanishing Fourier components only at the $\vec{G}$ vectors. If a monochromatic perturbation at $\vec{q}+\vec{G}'$ is switched on, the perturbed density has nonvanishing components at both sets, and the χ_0 matrix is obtained from the $\vec{q}+\vec{G}$ density components only. The $\vec{G}$ components of the perturbed density are equal to the unperturbed ones, within *linear* regime, but can be different because of quadratic and higher-order effects. So we obtain another accuracy check of the present method.

D. Brillouin-zone integration

The calculation of the electron density, for both the perturbed and unperturbed crystal, requires a BZ integration:

$$n(\vec{r})=2(2\pi)^{-3}\sum_{v}\int_{\mathrm{BZ}}d\vec{q}\,\langle\vec{r}\,|\,\vec{q},v\rangle\langle\vec{q},v\,|\,\vec{r}\rangle \tag{13}$$

and this is numerically performed with the mean-value points technique.[8–10] With an N-fold supercell, the BZ is folded back N times and the volume has a factor $1/N$, but there are N as many valence bands. The problem is that, in general, the set of special points depends upon the BZ shape and there is, in general, no guarantee that we will get the same accuracy for different N values. The choice of special points performed in this work does guarantee the same accuracy, and, even more, the doubled-cell results coincide exactly with the simple cell ones if a $\vec{q}=0$ perturbation is dealt with in both schemes.

To this aim we have used the reciprocal-space uniform orthogonal mesh of Monkhorst and Pack;[10] in their notation, we have chosen for the no-supercell case the (4,4,4) mesh. This gives 64 points in a cube but only 32 of them are not connected by a $\vec{G}$ vector and can be chosen in the fcc BZ. These are exactly the two Chadi-Cohen special points,[9] when all their symmetrically equivalent ones are separately considered (24 + 8). Of course, even at $\vec{q}=0$ the point symmetry of the crystal with built-in perturba-

tion is lower than the unperturbed crystal and the 32 points no longer reduce to two only. For the most unsymmetric perturbation, only time reversal can be invoked to reduce from 32 to 16.

When considering either the X or L supercells ($N=2$) simple geometrical considerations show that the new reciprocal vectors $\vec{q}+\vec{G}$ connect in both cases any of these 32 points to another point in the *same* set; therefore only 16 are now independent and can be chosen in the BZ of the superlattice; time reversal lowers this number further.

E. Independent elements

We use the same cutoff as in Refs. 7 and 11, i.e., all matrices (Hamiltonian, χ_0,ϵ) are set to zero when $|\vec{q}+\vec{G}|^2>21$ in $2\pi/a$ units. This gives a matrix size of 113×113 at Γ and of 108×108 at either X or L. But since the matrices are totally symmetric under the operations of the small point group of $\vec{q}$, the number of independent elements is reasonably small.

At the Γ point, the HDM is totally symmetric under all crystal symmetry operations and the body of it (i.e., $\vec{G}\neq0$ *and* $\vec{G}'\neq0$) has only 201 independent elements. These are separately evaluated within standard RPA in Refs. 7 and 11 using Eq. (11).[20] But according to the present method, we do *not* have to consider the response to 201 monochromatic perturbations, since each of them generates a whole column of χ_0, after Eq. (9). Looking more closely, the whole matrix can be built out of only one monochromatic perturbation per shell, i.e., 8 with the presently chosen cutoff (twice as many when separately considering sine and cosine, see Sec. III A).

At either the X or L points, the symmetry is lower and the number of independent elements higher. There are 468 of them at X and 598 at Γ; these can be built out of only 14 and 16 monochromatic perturbations, respectively.

IV. RESULTS

We present in this section the results obtained for the HDM's or Si and GaAs. For $\vec{q}=0$, standard RPA results to compare with have been obtained by Baldereschi and Tosatti[7] and by Resta and Baldereschi.[11] The problem of the BZ integration appearing in Eq. (11) has been widely discussed by these authors; the Chadi-Cohen two-point scheme[9] is the one to be chosen for the most meaningful comparison, being compatible with the scheme used here as explained in Sec. III D. We present in Table I the HDM elements calculated within direct and standard RPA for GaAs, with the same H_0 and the same cutoff. It is easily seen that the agreement between the two calculations is excellent, the absolute difference being of the order of 10^{-4}. Furthermore, from the several checks mentioned in the preceding section, we estimate the numerical accuracy of the present results to be at least 1 order of magnitude better. Therefore, we believe that most of the very small discrepancy is a convergence error of the standard RPA perturbation sums, which have been calculated in Refs. 7 and 11 summing over 90 conduction bands. For $\vec{q}$ at the zone boundary, at either X or L the standard

TABLE I. Hermitian dielectric matrix at $\vec{q}=0$ in GaAs. Only some of the independent elements are reported. The Resta and Baldereschi results, Ref. 11, shown in this table are those calculated with a two-point integration scheme (see text).

		This work		Resta and Baldereschi	
$\vec{G}$	$\vec{G}'$	Real	Imaginary	Real	Imaginary
111	111	1.6819	0.0000	1.6820	0
$\bar{1}11$	111	−0.0029	−0.0448	−0.0029	−0.0447
$1\bar{1}1$	$\bar{1}11$	−0.0142	0.0000	−0.0143	0
$1\bar{1}\bar{1}$	$\bar{1}11$	−0.1268	−0.0829	−0.1264	0.0830
200	111	0.1122	−0.0391	0.1123	−0.0390
200	$\bar{1}11$	0.0115	−0.0128	0.0112	−0.0128
200	200	1.5250	0.0000	1.5254	0
$\bar{2}00$	200	−0.0119	0.0000	−0.0117	0
020	200	−0.0093	0.0000	−0.0095	0

TABLE II. Hermitian dielectric matrix at the X point, $\vec{q}=(1,0,0)$ in units of $2\pi/a$. Only some of the independent elements are shown.

			GaAs	
G	G'	Si	Real	Imaginary
000	000	2.9484	2.8921	0.0000
$\bar{2}00$	000	0.0000	0.0000	0.4504
$\bar{1}1\bar{1}$	000	0.0829	0.1266	−0.0188
$\bar{1}1\bar{1}$	$\bar{1}1\bar{1}$	2.0860	2.0621	0.0000
002	$\bar{1}1\bar{1}$	−0.0022	−0.0006	0.0002
111	$\bar{1}1\bar{1}$	0.0185	−0.0010	0.0039
002	002	1.4198	1.4032	0.0000
022	002	−0.0065	−0.0038	0.0167
$1\bar{1}1$	$1\bar{1}1$	1.3305	1.3178	0.0000
111	$1\bar{1}1$	−0.0109	−0.0067	0.0192
200	$1\bar{1}1$	0.0532	0.0585	0.0181
022	022	1.1819	1.1796	0.0000
200	022	0.0146	0.0129	0.0048
$\bar{2}\bar{2}\bar{2}$	022	−0.0122	−0.0076	0.0094

TABLE III. Hermitian dielectric matrix at the L point, $\vec{q}=(\frac{1}{2},\frac{1}{2},\frac{1}{2})$ in units of $2\pi/a$. Only some of the independent elements are shown.

			GaAs	
G	G'	Si	Real	Imaginary
000	000	3.1683	3.0854	0.0000
$\bar{1}\bar{1}\bar{1}$	000	0.7425	0.6818	0.4391
$\bar{2}\bar{2}\bar{2}$	000	−0.1393	−0.1425	−0.0198
$\bar{1}1\bar{1}$	$\bar{1}1\bar{1}$	1.7969	1.7971	0.0000
$\bar{2}00$	$\bar{1}1\bar{1}$	0.1095	0.1443	−0.0543
111	$\bar{1}1\bar{1}$	0.0232	0.0083	0.0023
$\bar{1}11$	$\bar{1}11$	1.4290	1.4200	0.0000
002	$\bar{1}11$	0.0628	0.0739	0.0215
$\bar{2}02$	$\bar{1}11$	0.0551	0.0648	−0.0181
002	002	1.2775	1.2737	0.0000
111	002	0.0532	0.0617	0.0185
$\bar{1}\bar{1}3$	002	−0.0087	−0.0018	−0.0047
111	111	1.2711	1.2693	0.0000
$\bar{2}\bar{2}\bar{2}$	111	−0.0197	−0.0064	0.0153
$\bar{2}02$	111	0.0157	0.0128	0.0027

RPA of Refs. 7 and 11 becomes computationally rather heavy, and we have no complete results to compare with. In this work, we have calculated the HDM of Si and GaAs both at the X and L points; some independent elements are shown in Tables II and III.

The diagonal elements $\tilde{\epsilon}(\vec{q}+\vec{G},\vec{q}+\vec{G})$ are a smooth function of $\vec{q}+\vec{G}$, decreasing towards 1 with increasing $|\vec{q}+\vec{G}|$. The other HDM elements are numbers where trends and physical meanings are hardly detectable—a feature noticed several times.[1,3,7,11] Their significance becomes clear when applied to screen specific perturbations. An overall look is most meaningfully obtained with a DBS analysis, which is performed in Sec. V.

V. DIELECTRIC BAND STRUCTURE

Like any Hermitian operator, the HDM can be diagonalized. The eigenvectors at a given $\vec{q}$ point are a type of normal coordinates in the screening problem, and have no direct link to real physical perturbations. Nevertheless, this concept of DBS, proposed some years ago by Baldereschi and Tosatti[18] is a nice mathematical tool to extract some important trends from the HDM's. At high-symmetry $\vec{q}$ points the HDM eigenvalues can be classified according to the small group of $\vec{q}$, and the symmetry of the most screened perturbations is straightforwardly visualized. For instance, trends with increasing ionicity for the isoelectronic series Ge-GaAs-ZnSe have been identified and their origin has been understood[11] through a DBS analysis. When dealing with one material, but several different HDM models, the DBS gives a kind of fingerprint of the main screening features of each model. In the case of Si, a very detailed study has been published by Car *et al.*[22] with reference to some of the existing models.[22–24]

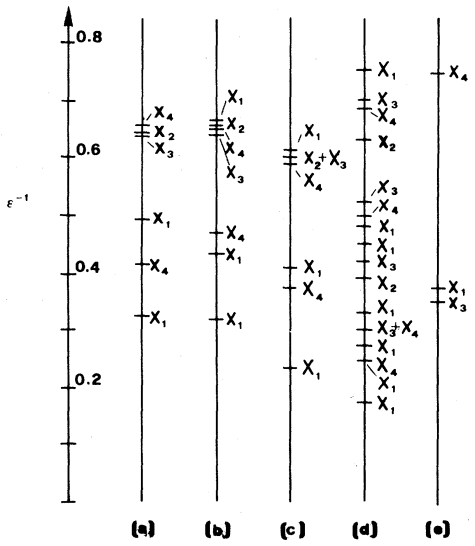

FIG. 1. Eigenvalues of the inverse HDM at the X point in Si. (a): Present work; (b): Car-Selloni (Ref. 24); (c): local-density model (Ref. 21); (d): Johnson model (Ref. 23); and (e): Sinha model (Ref. 22). Calculations (b), (c), (d), and (e) are taken from Ref. 21.

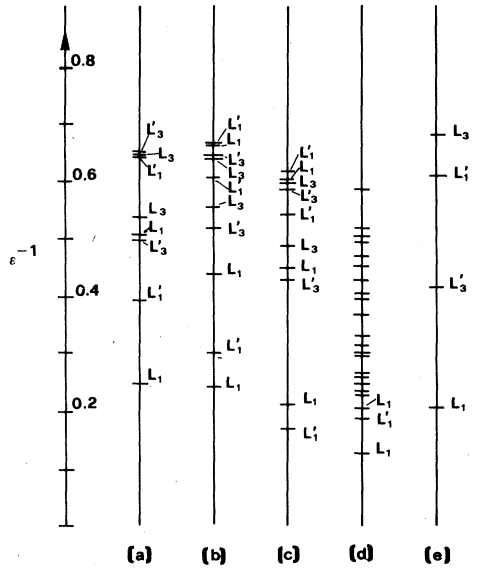

FIG. 2. Eigenvalues of the inverse HDM at the L point in Si. (a)—(e) represent different models as in Fig. 1.

Before this work, first-principles results were only available at $\vec{q}=0$ or $\vec{q}\to 0$; therefore at finite-q values Car *et al.* were only allowed to compare different models between themselves. In this section, we augment their analysis by comparing at the X and L points the model results with the present first-principle ones for Si. The results are presented in Figs. 1 and 2, where the most screened eigenvalues of $\tilde{\epsilon}^{-1}$ are shown.

It can be seen that the model which looks overall most similar to the first-principle result is the Car-Selloni model,[24] even if the ordering of the eigenvalues is partly different. This is not surprising, since this model has been fitted after the first-principle HDM of Ref. 7, while the other ones have been proposed for a "specialized" use in lattice dynamics. In order to calculate phonon frequencies, only a limited amount of the information embedded in the HDM is used. Some models are able to predict good frequencies, although being strongly unsatisfactory for the physics of the screening process as a whole. The reasons why have been investigated in much detail by Car *et al.*,[21] to whom we refer to for a discussion on this point. In addition, we only wish to point out the fact that a typical fingerprint of local-field effects is the gap between the two most screened eigenvalues at the L point, since a diagonal HDM has an "empty lattice" DBS, and a closed gap. The Car-Selloni model gives the right ordering of levels, although it underestimates the L gap. In general, both the Car-Selloni and the local-density[21] models underestimate local-field effects, while Sinha's model[22] overestimates them. The Johnson model[23] is strongly unphysical, as already realized by Car *et al.*[21]

VI. DISCUSSION AND CONCLUSIONS

In this work we have presented a novel approach to calculate first-principle dielectric matrices in solids. The main limitations of the standard RPA, as applied to real

solids and realistic band structures, are overcome by our direct RPA methods, which allows much simpler computations without losing accuracy. One of the features making the present method very appealing is that we are able to get the fully converged perturbation sum without actually summing over empty states, while the standard RPA requires explicitly dealing with very high conduction bands.[7,11] The problem of slowly convergent perturbation sums, indeed, was recently circumvented also by Van Camp *et al.*[25] who used a moment expansion approach, but since their expansion is actually cut at a given order, the numerical results only approximate the RPA value.[6] On the contrary, we have shown here that we can easily obtain numerically the exact standard RPA results.

In this first application of the method, we have calculated the RPA dielectric matrices of Si and GaAs, with the use of Cohen-Bergstresser[17] band structure, in order to closely compare with previously published standard RPA calculations.[7,11,18] Besides reproducing them, we are now able to extend beyond; the results reported in Tables II and III and in Figs. 1 and 2, therefore, supplement those of Refs. 7, 11, and 18.

The shortcomings of the present approach are exactly the same as in any calculation based on supercell techniques.[13,14] The system (crystal plus perturbation) must have a periodicity which is commensurate to the unperturbed lattice. The supercell size cannot be arbitrarily large, but within the present computational possibilities, the attainable $\vec{q}$ points in the BZ form a mesh which is dense enough in order to interpolate or extrapolate[26] the HDM elements. There is presently a need for simple and yet realistic HDM models; *ab initio* calculations within the present methods can provide a reference frame for them.

Finally we briefly outline the possible extension of the method beyond RPA. Suppose we know the self-consistent one-electron potential obtained for the *unperturbed* crystal within the LDF scheme.[14–16] Then our approach yields the independent-electron polarizability χ_0; the LDF dielectric matrix is then related to this χ_0 by a relationship which is not the simple RPA one, but which is nevertheless tractable and easily implementable.[13,19] Notice that χ_0 is obtained here through ground-state calculations for the crystal with a frozen-in perturbation, but these must *not* be self-consistent. This is an important new feature of our method: To the best of our knowledge, all of the existing direct LDF treatments of perturbed crystals *do* require self-consistency for each perturbation considered. We are referring here to frozen phonons[12] and generalizations,[13–16] as well as to very recent work on dielectric screening.[4,26] A direct evaluation of the inverse HDM, having several features related to the present work but based on self-consistent LDF calculations, is presently being performed by Kunc and Tosatti.[27]

ACKNOWLEDGMENTS

We have benefited from discussions with A. Baldereschi, K. Kunc, and E. Tosatti. We also wish to thank K. Kunc and E. Tosatti for communicating to us some of their preliminary results.[27]

*To whom correspondence should be addressed.

[1]A. Baldereschi, in *Proceedings of the XV International Conference on the Physics of Semiconductors, Kyoto, 1980* [J. Phys. Soc. Jpn. **49**, Suppl. A155 (1980)].

[2]*Ab-Initio Calculation of Phonon Spectra,* edited by J. T. Devreese, V. E. Van Doren, and P. E. Van Camp (Plenum, New York, 1983).

[3]A. Baldereschi and R. Resta, in Ref. 2, p. 1.

[4]K. Kunc and R. Resta, Phys. Rev. Lett. **51**, 686 (1983).

[5]S. L. Adler, Phys. Rev. **126**, 413 (1962); N. Wiser, *ibid.* **129**, 62 (1963).

[6]P. E. Van Camp, V. E. Van Doren, and J. T. Devreese, in Ref. 2, p. 24.

[7]A. Baldereschi and E. Tosatti, Phys. Rev. B **17**, 4710 (1978).

[8]A. Baldereschi, Phys. Rev. B **7**, 5212 (1973).

[9]D. J. Chadi and M. L. Cohen, Phys. Rev. B **8**, 5747 (1973).

[10]H. J. Monkhorst and J. D. Pack, Phys. Rev. B **13**, 5188 (1976).

[11]R. Resta and A. Baldereschi, Phys. Rev. B **23**, 6615 (1981).

[12]H. Wendel and R. M. Martin, Phys. Rev. B **19**, 5251 (1979); Festkoerperprobleme **19**, 21 (1979).

[13]R. M. Martin and K. Kunc, in Ref. 2, p. 49.

[14]K. Kunc and R. M. Martin, in Ref. 2, p. 65.

[15]K. Kunc and R. M. Martin, Phys. Rev. Lett. **48**, 406 (1982).

[16]K. Kunc, Helv. Phys. Acta **56**, 559 (1983).

[17]M. L. Cohen and T. K. Bergstresser, Phys. Rev. **141**, 789 (1966).

[18]A. Baldereschi and E. Tosatti, Solid State Commun. **29**, 131 (1979).

[19]P. E. Van Camp, V. E. Van Doren, and J. T. Devreese, Phys. Rev. B **24**, 1096 (1981); Phys. Status Solidi B **110**, K133 (1982).

[20]The independent elements evaluated in Refs. 7 and 11 in the $\vec{q}\rightarrow 0$ limit are actually 217. This figure comes out from nonanalytic "wing" ($\vec{G}=0$) elements. For an analytic matrix, the independent elements are $201+8+1=210$.

[21]R. Car, E. Tosatti, S. Baroni, and S. Leelaprute, Phys. Rev. B **24**, 985 (1981).

[22]S. K. Sinha, Phys. Rev. **177**, 1256 (1969).

[23]D. L. Johnson, Phys. Rev. B **9**, 4475 (1974).

[24]R. Car and A. Selloni, Phys. Rev. Lett. **40**, 1365 (1979).

[25]P. E. Van Camp, V. E. Van Doren, and J. T. Devreese, Phys. Rev. Lett. **42**, 1224 (1979).

[26]J. B. McKitterick, Phys. Rev. B **28**, 7384 (1983).

[27]K. Kunc and E. Tosatti, Phys. Rev. B **29**, 7045 (1984).